applied sciences

MDPI

Article

Development and Evaluation of a Prototype Scratch Apparatus for Wound Assays Adjustable to Different Forces and Substrates

Roman Grimmig, Patrick Babczyk, Philipp Gillemot, Klaus-Peter Schmitz, Margit Schulze * and Edda Tobiasch *

Department of Natural Sciences, Bonn-Rhein-Sieg University of Applied Sciences, von-Liebig-Strasse 20, D-53359 Rheinbach, Germany; roman.grimmig@h-brs.de (R.G.); patrick.babczyk@h-brs.de (P.B.); philipp.gillemot@h-brs.de (P.G.); klaus-peter.schmitz@h-brs.de (K.-P.S.)

* Correspondence: margit.schulze@h-brs.de (M.S.); edda.tobiasch@h-brs.de (E.T.)

Received: 27 August 2019; Accepted: 15 October 2019; Published: 18 October 2019

Abstract: Scratch assays enable the study of the migration process of an injured adherent cell layer in vitro. An apparatus for the reproducible performance of scratch assays and cell harvesting has been developed that meets the requirements for reproducibility in tests as well as easy handling. The entirely autoclavable setup is divided into a sample translation and a scratching system. The translational system is compatible with standard culture dishes and can be modified to adapt to different cell culture systems, while the scratching system can be adjusted according to angle, normal force, shape, and material to adapt to specific questions and demanding substrates. As a result, a fully functional prototype can be presented. This system enables the creation of reproducible and clear scratch edges with a low scratch border roughness within a monolayer of cells. Moreover, the apparatus allows the collection of the migrated cells after scratching for further molecular biological investigations without the need for a second processing step. For comparison, the mechanical properties of manually performed scratch assays are evaluated.

Keywords: wound healing assay; scratch assay; cell harvesting; cell migration; prototype apparatus; endothelial cells

1. Introduction

As the outer shell of the human body, skin forms the human's largest organ [1]. When skin is injured, it is able to repair itself while passing through five stages of wound healing: haemostasis, inflammation, proliferation, migration, and maturation [2,3]. As a part of this process, cells migrate into the wounded area [4]. Wound healing assays can be set up in order to enable further investigation of the skin wound-healing process in vitro [5–7].

The popularity of these assays can be explained by the simplicity of their procedures. In such procedures, a layer of adherent cells is wounded under specified conditions and the subsequent migration of the contiguous cells into the fresh and cell-free area is observed and analyzed [8–10]. Such a defined cell layer can be wounded by scratching, stamping using PDMS or neoprene [11–13], thermal wounding [14], electrical wounding [15], or optical wounding [16,17]. Scratching is most commonly performed in well plates using pipette tips [18–20]. However, it can also be performed by using a variety of sharp-edged tools like toothpicks [21], metallic micro-indenters [22], or cell scrapers [23].

Furthermore, it is reported that scratches are performed on coverslips, which can be placed into a 6-well plate [24]. In other techniques, inlets within dishes or wells to create a cell free area have been used [25]. The general aim of a scratch assay is to provide straight borders in a reproducible

way without damaging cells [26]. However, the reproducibility of manually performed scratch assays strongly depends on the performer and their skills [27].

An attachment for forceps-like scrapers to create scratches of defined direction, length, width, and depth in 6-well plates has been developed to investigate keratinocyte migration [28]. Scratches obtained with this scratch stencil are reported to be inflicted with high precision and in a reproducible fashion [29]. The material chosen by this group, polyoxymethylene, is generally a suitable construction material in concerns of laboratory apparatus construction [30].

In all aforementioned strategies, it is only possible to investigate the migration behavior of cells under different conditions. Subsequent molecular biological investigations using RNA or protein samples from migrated cells were impossible due to the fixation of the cells. Therefore, migration assays were performed separately by using transwell or Boyden chambers. After migration, the migrated cells were collected for further investigations [31–33].

Depending on the needs of experimental design and availability, the used cell types for the mentioned investigation methods of migration and wound healing may vary. For instance, to study epithelial repair, epithelial cells from the lung [34] or the retina [35] are commonly used. Another interesting source is represented by mesenchymal stem cells, which can be differentiated towards multiple cell types [36–42]. Setiawan and colleagues even differentiated human adipose-derived stem cells towards epithelial cells for usage in scratch assays [43]. Fibroblasts from foreskin (HFF), skin (HDF), or nasal polyps (NPDF) have recently been used as well as microglia cells and keratinocytes [25,44–46]. In addition to the mentioned cell types, endothelial cells are a favorable source to study migration. Many working groups used either human or bovine endothelial cells in scratch assays and other migration assays [47–56].

This study covers the development and evaluation of a prototype scratch apparatus for wound assays, focusing on the comparison to conventional procedures. The presented device allows for the collection of migrated cells after scratching for further investigations, without the need of a second processing step. Moreover, the apparatus is adjustable in angle, normal force, shape, and material to adapt to a specific question and demanding substrates. In detail, scratching performance is examined for different configurations to identify parameters leading to an ideal scratch.

2. Experimental Section

2.1. Characterization of Manually and Automatically Performed Scratch Assays

As a model culture, HMEC-1 (ATCC, Manassas, VA, USA) cultivated in 60 mm petri dishes (Sarstedt, Nümbrecht, Germany) was used in all experiments.

For manually performed scratch assays using pipette tips (Sarstedt, Nümbrecht, Germany), rubber spatulas (Deutsch & Naumann, Berlin, Germany) and cell scrapers (Sarstedt, Nümbrecht, Germany), the recommended procedures according to [8,57] were followed. A swift and consistent scratch of 30 mm length was applied to the culture dish surface. Every scratch assay was performed in a sixfold determination.

For the scratching device, normal angles varied between +/−45°, normal forces varied from 0.3 to 1.0 N/scratch, and the directions varied concerning push and pull performance. The control of the force impacting the cell substrate was achieved using calibrated weights mounted to the scratch head. Acting force was acquired using a calibrated load cell (VWR, Radnor, PA, USA) beneath the culture dish. Image processing was performed using OriginPro 2017 (Originlab, Northhampton, MA, USA). The scratching performance is considered as the roughness of the scratch edge obtained, expressed as the mean deviation from its linear regression (Figure 1). In order to identify and classify the parameters leading to an optimal scratch, median values are processed as they are less prone to severe deviations in the overall measurement.

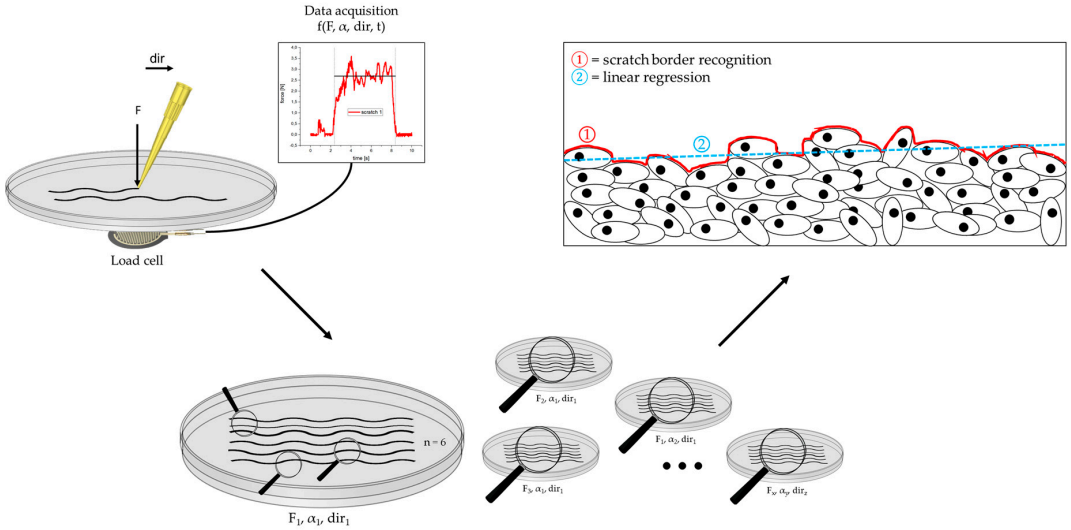

Figure 1. Scheme of the data acquisition. In the first step, acting forces are collected in a variety of experimental configurations. Secondly, each scratching setup (F, α, dir) is evaluated microscopically in a sixfold determination. Finally, the obtained pictures are processed concerning the scratch border recognition and subsequent regression for roughness quantification.

2.2. Evaluation of the Harvesting Capabilities of the Scratch Device

A monolayer of cells was grown (60 mm culture dish, cell density: 200,000 cells/dish, medium: DMEM + 10% FBS), scratched and re-scratched using only one culture dish. To increase the number of scratch edges, 30 mm blades made from standard cell culture scrapers (Sarstedt, Nümbrecht, Germany) with set-in jags were used. After scratching under different tested conditions, the cells were allowed to migrate for 24 h at 37 °C in the incubator. The dishes were mounted in the device and marked to set the correct orientation for re-scratching and microscopic assessment. To evaluate the migration capacity of the cells using a Zeiss Axio Observer D.1 microscope (Oberkochen, Germany) and AxioVision software, the dishes were placed onto a dish- and slide-holder at the set orientation before and after incubation. For facilitated and accurate microscopic determination of the migration behavior, the pre-scratched coordinates within the culture dish were re-approached after scratching.

3. Results and Discussion

3.1. Conception and Construction of the Apparatus

In order to meet the requirements for both reproducibility and easy handling, a simple mechanical apparatus was designed. The overall requirements for this device, which can be considered a laboratory or even medical product, include an operation at room temperature, contact to cell cultures, cleaning in a conventional laboratory washer, sterilization in an autoclave, and portability [58].

The device itself was designed to be completely disassemblable and to be easily manufactured by a common milling machine and lathe. It consists of two modular parts to fulfil the function of the sample scratching and locomotion, respectively (Figure 2).

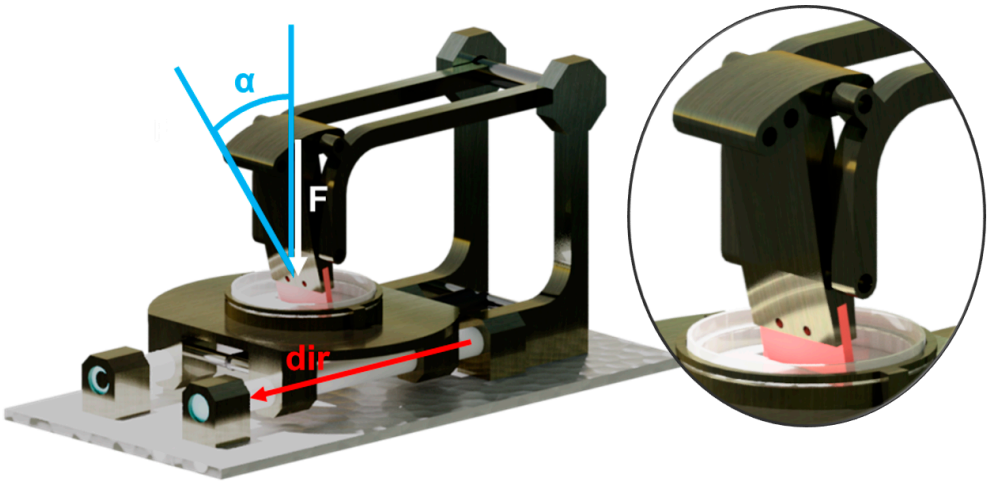

Figure 2. 3D model of the constructed apparatus consisting of two main components: while the sample translation system (front) ensures track accuracy, the actual scratching system (back/top) enables different angles and forces for the scratching blade (depicted in red). The parameters under investigation are highlighted.

The scratching part of the device needs to scratch a cell substrate of undefined thickness from above in different, defined angles with respect to the sample surface [18,57,59,60]. The scratching blade should be disposable or at least replaceable and changeable in geometry for multiple simultaneous scratches. Moreover, the force impacting on the sample should be able to be varied as different cell cultures are known to show diverging adhesion forces.

This has been realized by a T-shaped scratch head that can mount any suitable construction material (e.g., polymers) with a thickness of 2 mm. The blade is fixed in position by two threaded shafts. The scratch head itself can be adjusted by rotating around the lower axis and fixed in five positions. Two extension arms, fixed to a polytetrafluoroethylene (PTFE) bushed axle, enable the head to be lifted up for sample exchange or revision. In order to tune the normal force impacting on the sample surface, additional weights can be attached. The rear mounting brackets also feature an axle that allows mounting a gas spring for an automated sample locomotion. Stainless steel was chosen for the axles and aluminum alloy for all other construction parts.

The sample locomotion part of the device needs to suppress culture dish rotation, tilting, as well as undesired axial and radial movements. Additionally, the actual locomotion should be automated, smooth, directionally stable under force impact, easy to handle and to release, and ensure maximum accuracy.

This is solved by the construction of a linear slide. The sled guide consists of a PTFE sleeved stainless steel rod on which the sled's brackets can glide. The sample holder plate provides an annular culture dish holder with a bayonet type lock that secures the culture dish.

3.2. Comparison of Manually and Automatically Performed Scratching

In order to evaluate the capabilities and limitations of the scratching performances, the scratch border roughness is interpreted as a function of its respective operating procedure. For manually, as well as automatically performed scratch assays, the impacting forces and the border roughness values are depicted (Figure 3).

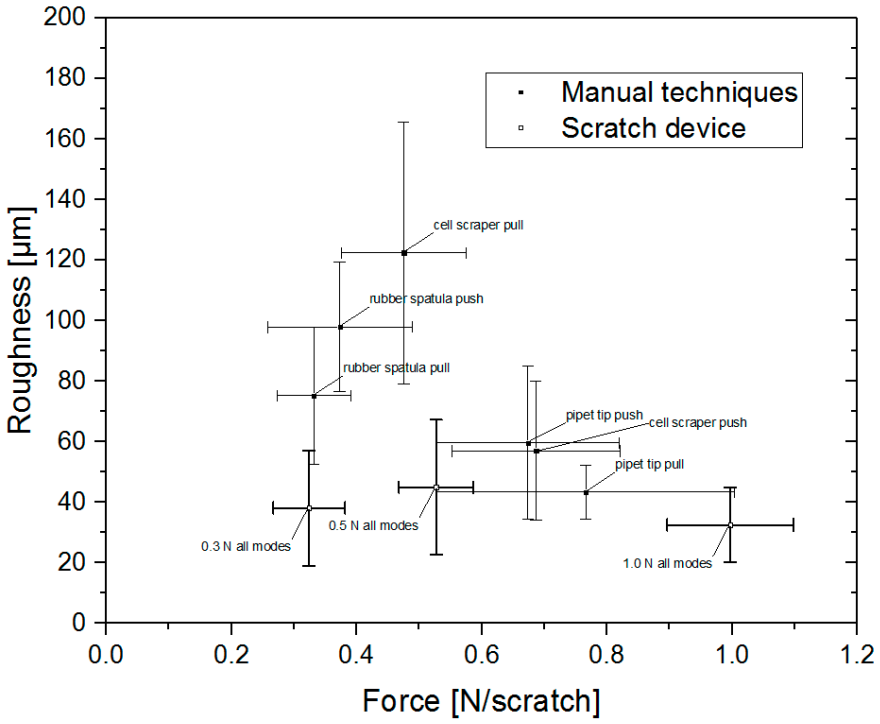

Figure 3. Comparison of manually performed scratch assays versus assays performed with the scratch device (thick lines). Nearly independent from its operation mode, the scratch device achieves scratch borders that show a lower roughness than many conventional methods that allow cell harvesting.

It shows that manually and automatically performed roughness values vary depending on their operational mode and especially on the method used. While the manually performed values range between 30 and 170 µm, the mechanically performed scratches enable values of 20 to 70 µm. Concerning the force accuracy, the manually performed assays vary by roughly 0.1 to 0.15 N per scratch and exceed 0.2 N per scratch for the usually favoured pipette tip technique. Mechanically performed scratch assays undergo a variation of less than 0.1 N/scratch, even with the directional mode not being differentiated.

When taking a closer look at the manually performed scratch techniques, the force deviation depends on the tool used. While the rigid and barely deformable pipette tip shows a large force deviation due to the operator guiding it, the rubber spatula and cell scraper perform with little deviation. Both these elastic tools show a more rigid and therefore inconsistent force application in push direction; however, in pull direction deviations can be smoothed out more easily. Concerning the automated scratching, the deviation in force results from the simultaneous consideration of push and pull assays.

At this point, it can be stated that the conventionally used pipette tip provides the scratching border with the least roughness values of all manual techniques investigated.

3.3. Comparison of Different Operational Settings Using the Scratch Device

As a low roughness value was desired, a closer differentiation of the influencing parameters on the mechanically produced scratch borders was carried out. A classification of all experimental data into the varied parameters via box plot (Figure 4) revealed that there are distinct settings for direction, force, and angle that lead to lower mean and median values for optimum scratch performance.

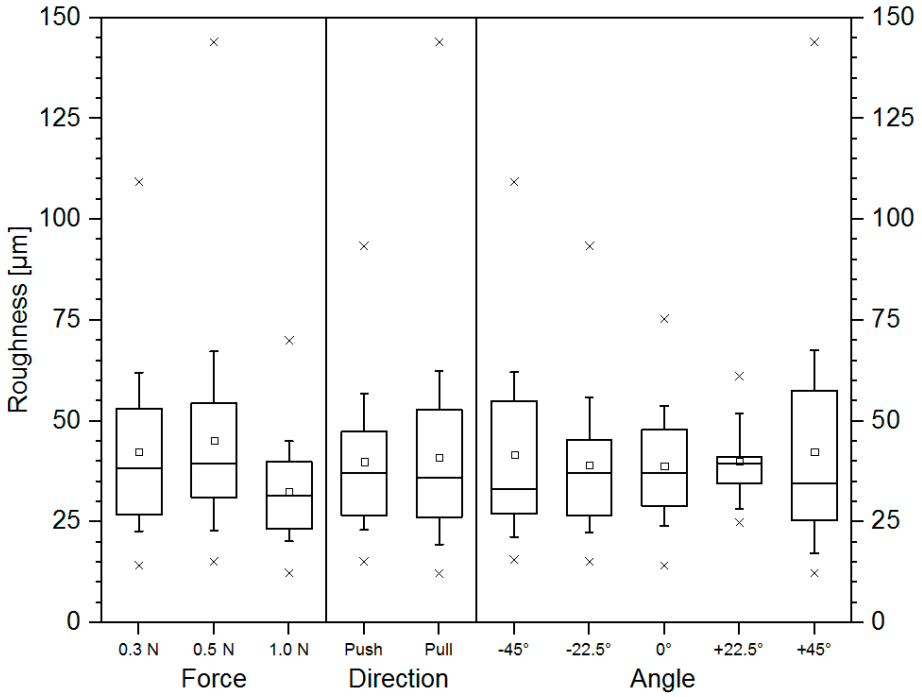

Figure 4. Roughness values obtained during the scratch performances, unfiltered and classified into their respective configuration (force, direction, and angle), displayed as a box plot (symbols: □ = mean value, x = min/max values). It is possible to visually identify operational modes that have enabled reliable scratch borders with a low border roughness.

As the order of classification plays an important role [61,62], the three classification parameters (angle, direction, and force) have been checked for the lowest roughness median value in all six possible decision tree permutations (Figure 5).

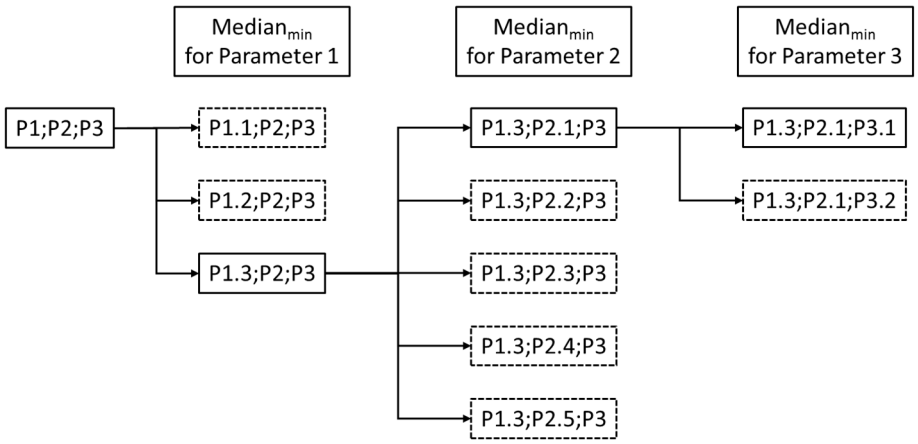

Figure 5. Construction of the decision trees for the classification of the roughness data. The order of the refinement parameters is permuted to obtain all possible outcomes independently from each other.

A subsequent evaluation of the step-wise refinement for the ideal parameters (Figure 6) shows a probability for achieving a low scratch border roughness.

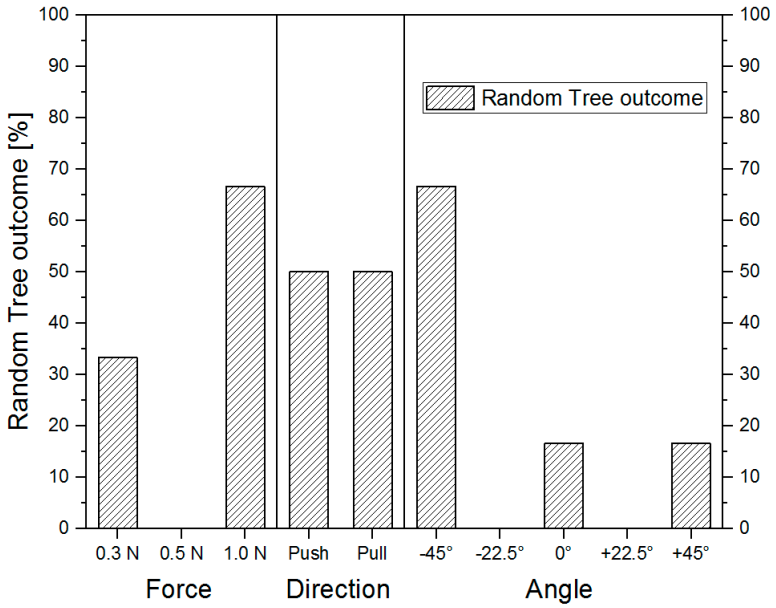

Figure 6. With all decision trees simulated, the resulting outcomes can be evaluated. For the best scratching results via scratch device, the scratching direction can be neglected whereas high scratching forces (1.0 N) and a specific angle (−45°) are favored.

When the highest force is applied, a good scratch is deemed the most probable. A chosen angle of −45° also leads to a desirable outcome of the scratch border. Concerning the scratching direction, no preference was observed.

As to the refinement of the scratching parameters, the outcome represents a probability to achieve a good scratch border (meaning a low roughness value). As the outcome of the scratch direction shows a 50% distribution for every direction, the influence can be considered inessential. A different picture can be drawn when the applied force and scratching angle are considered. In four out of six decision trees, the best outcomes have been recorded for the highest force applied. This is in accordance with the manual scratch techniques, which also obtained smoother scratch borders when a reasonably high force was applied. In the range of the results observed, the application of 0.5 N force per scratch had to be avoided.

3.4. Perfomance of the Automated Scratch Assays on the Harvesting Capabilities

As shown before, the pipette tip technique as a quick scratch assay tool has its justification for good reason. However, the advantages of easy handling and a good scratch border are outmatched by the fact that the pipette tip is the only technique investigated that is incapable of scratching (Figure 7A) and re-scratching (=harvest) migrated (Figure 7B) cells. In contrast, by using the scratch device, a clear and linear scratch edge was created (Figure 7C). Cells that migrated into the scratch within 24 h (Figure 7D) were collected by re-scratching the same position (Figure 7E).

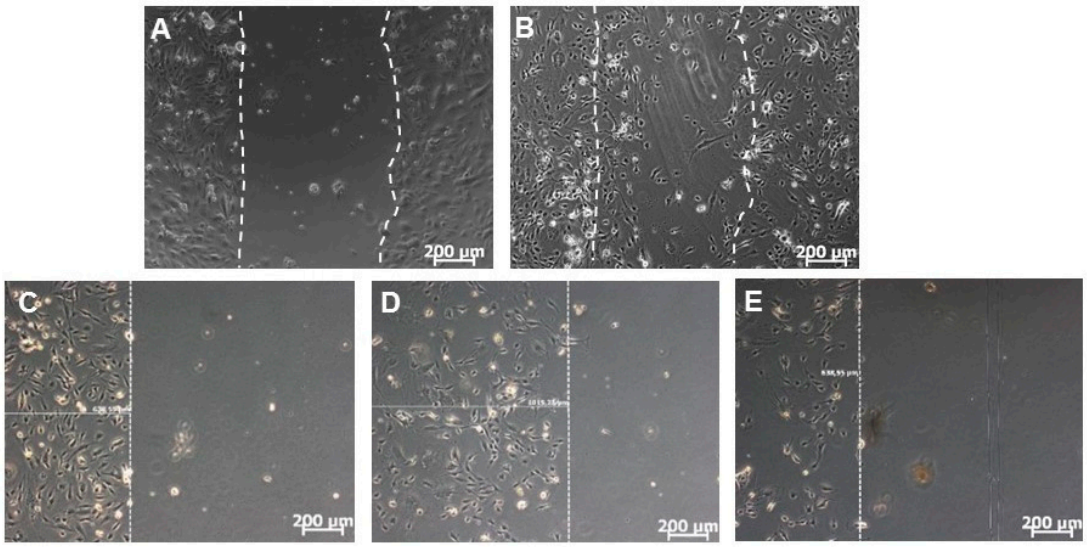

Figure 7. Comparison of conventional scratch assay versus scratch device. Cells were scratched with a 100 µL pipette tip (**A**) and cells migrated into the scratch within 24 h (**B**). By using the device, a clear and linear scratch was created (**C**) and the cells migrated into the scratch within 24 h (**D**). After the migration, the cells were re-scratched and collected at the same position (**E**).

4. Conclusions

The need for a simple device for the performance of reproducible scratch assays including harvesting was met by the construction of an apparatus that consisted of a modular setup featuring a sample scratching and a sample locomotion system. The design was kept simple to enable both individual adjustment in force, angle, and direction. The conducted experiments show that scratch borders were generated, which were straighter and more reproducible than manually performed assays. Concerning both manually and automatically performed assays, the lowest scratch border roughness data were obtained when using high forces on the substrate.

In contrast to conventional methods, which include a two-step model of scratch assays in well plates and a subsequent migration assay in transwell chambers or Boyden chambers, the presented scratch device simplifies the procedure into just a single step. In conclusion, this apparatus is suitable for facilitated microscopic monitoring of cell migration and proliferation and enables the harvesting and investigation of these cells only.

Author Contributions: Data curation (apparatus design and construction and experiments regarding the mechanical scratching performance) and writing/original draft preparation, R.G.; data curation (cell culture experiments) and writing/original draft preparation, P.B.; data analysis and writing, P.G.; methodology and resources, K.-P.S.; writing/review and editing, M.S.; conceptualization, methodology, supervision, review, and editing, E.T.

Funding: This work was supported and financed by the Federal Ministry of Education and Research program "FHprofUnt" project "MeMoAthero" (grant number: 03FH012PB2). A PhD scholarship was given to P.B. by the Graduate Institute of the Bonn-Rhein-Sieg University of Applied Sciences.

Acknowledgments: We gratefully thank Debora Turetsky (Northwestern University, Evanston, Illinois, U.S.) for English corrections.

Conflicts of Interest: The authors declare no conflict of interest.

References

1. Kanitakis, J. Anatomy, histology and immunohistochemistry of normal human skin. *Eur. J. Dermatol.* **2002**, *12*, 390–401. [PubMed]
2. Boateng, J.; Catanzano, O. Advanced Therapeutic Dressings for Effective Wound Healing—A Review. *J. Pharm. Sci.* **2015**, *104*, 3653–3680. [CrossRef] [PubMed]

3. Sorg, J.M.R.H. Wound Repair and Regeneration. *Eur. Surg. Res.* **2012**, *49*, 35–43.
4. Lampugnani, M.G. Cell Migration into a Wounded Area In Vitro. In *Adhesion Protein Protocols*; Humana Press: Totowa, NJ, USA, 1999; pp. 177–182.
5. Rodriguez, L.G.; Wu, X.; Guan, J.-L. Wound-Healing Assay. In *Cell Migration: Developmental Methods and Protocols*; Guan, J.-L., Ed.; Humana Press: Totowa, NJ, USA, 2005; pp. 23–29. ISBN 978-1-59259-860-1.
6. Stamm, A.; Reimers, K.; Strauß, S.; Vogt, P.; Scheper, T.; Pepelanova, I. In vitro wound healing assays - State of the art. *BioNanoMaterials* **2016**, *17*, 79–87. [CrossRef]
7. Pijuan, J.; Barceló, C.; Moreno, D.F.; Maiques, O.; Sisó, P.; Marti, R.M.; Macià, A.; Panosa, A. In vitro Cell Migration, Invasion, and Adhesion Assays: From Cell Imaging to Data Analysis. *Front. Cell Dev. Biol.* **2019**, *7*, 1–16. [CrossRef]
8. Liang, C.; Park, A.Y.; Guan, J. In vitro scratch assay: A convenient and inexpensive method for analysis of cell migration in vitro. *Nat. Protoc.* **2007**, *2*, 329–333. [CrossRef]
9. Silva Nunes, J.P.; Martins Dias, A.A. ImageJ macros for the user-friendly analysis of soft-agar and wound-healing assays. *Biotechniques* **2017**, *62*, 175–179. [CrossRef]
10. Vargas, A.; Angeli, M.; Pastrello, C.; Mcquaid, R.; Li, H.; Jurisicova, A.; Jurisica, I. Robust quantitative scratch assay. *Bioinformatics* **2016**, *32*, 1439–1440. [CrossRef]
11. Lan, R.; Geng, H.; Hwang, Y.; Mishra, P.; Skloss, W.L. A novel wounding device suitable for quantitative biochemical analysis of wound healing and regeneration of cultured epithelium. *Wound Repair Regen.* **2010**, *18*, 159–167. [CrossRef]
12. Fong, E.; Tzlil, S.; Tirrell, D.A. Boundary crossing in epithelial wound healing. *Proc. Natl. Acad. Sci. USA* **2010**, *107*, 19302–19307. [CrossRef]
13. Nikolić, D.L.; Boettiger, A.N.; Bar-Sagi, D.; Carbeck, J.D.; Shvartsman, S.Y. Role of boundary conditions in an experimental model of epithelial wound healing. *Am. J. Physiol. Cell Physiol.* **2006**, *291*, 68–76. [CrossRef] [PubMed]
14. Hettler, A.; Werner, S.; Eick, S.; Laufer, S.; Weise, F. A New In Vitro Model to Study Cellular Responses after Thermomechanical Damage in Monolayer Cultures. *PLoS ONE* **2013**, *8*, e82635. [CrossRef] [PubMed]
15. Giaever, I.; Keese, C.R. Micromotion of mammalian cells measured electrically. *Proc. Natl. Acad. Sci. USA* **1991**, *88*, 7896–7900. [CrossRef] [PubMed]
16. Zordan, M.D.; Mill, C.P.; Ii, D.J.R.; Leary, J.F. A High Throughput, Interactive Imaging, Bright-Field Wound Healing Assay. *Cytom. Part A* **2011**, *79*, 227–232. [CrossRef] [PubMed]
17. Song, Q.; Uygun, B.; Banerjee, I.; Nahmias, Y.; Zhang, Q.; Berthiaume, F.; Latina, M.; Yarmush, M.L. Low power laser irradiation stimulates the proliferation of adult human retinal pigment epithelial cells in culture. *Cell. Mol. Bioeng.* **2009**, *2*, 87–103. [CrossRef]
18. Grada, A.; Otero-Vinas, M.; Prieto-Castrillo, F.; Obagi, Z.; Falanga, V. Research Techniques Made Simple: Analysis of Collective Cell Migration Using the Wound Healing Assay. *J. Invest. Dermatol.* **2017**, *137*, e11–e16. [CrossRef]
19. Menger, B.; Vogt, P.M.; Allmeling, C.; Radtke, C. AmbLOXe—An Epidermal Lipoxygenase of the Mexican Axolotl in the Context of Amphibian Regeneration and Its Impact on Human Wound Closure In Vitro. *Ann. Surg.* **2011**, *253*, 410–418. [CrossRef]
20. Bennett, J.; Cassidy, H.; Slattery, C.; Ryan, M.; McMorrow, T. Tacrolimus Modulates TGF-β Signaling to Induce Epithelial-Mesenchymal Transition in Human Renal Proximal Tubule Epithelial Cells. *J. Clin. Med.* **2016**, *5*, 50. [CrossRef]
21. Klettner, A.; Tahmaz, N.; Dithmer, M.; Richert, E.; Roider, J. Effects of aflibercept on primary RPE cells: Toxicity, wound healing, uptake and phagocytosis. *Br. J. Ophthalmol.* **2014**, *98*, 1448–1452. [CrossRef]
22. Topman, G.; Sharabani-yosef, O.; Gefen, A. Medical Engineering & Physics A standardized objective method for continuously measuring the kinematics of cultures covering a mechanically damaged site. *Med. Eng. Phys.* **2012**, *34*, 225–232.
23. Baudin, B.; Bruneel, A.; Bosselut, N.; Vaubourdolle, M. A protocol for isolation and culture of human umbilical vein endothelial cells. *Nat. Protoc.* **2007**, *2*, 481–485. [CrossRef] [PubMed]
24. Molladavoodi, S.; Wulff, D.; Robichaud, M.; Gorbet, M. Corneal epithelial cells exposed to shear stress show altered cytoskeleton and migratory behaviour. *PLoS ONE* **2017**, *12*, e0178981. [CrossRef] [PubMed]

25. Tang, Y.; Cui, Y.; Li, Z.; Jiao, Z.; Zhang, Y.; He, Y.; Chen, G.; Cheng, G.; Zhou, Q.; Wang, W.; et al. Radiation-induced miR-208a increases the proliferation and radioresistance by targeting p21 in human lung cancer cells. *J. Exp. Clin. Cancer Res.* **2016**, *35*, 7. [CrossRef] [PubMed]
26. Kramer, N.; Walzl, A.; Unger, C.; Rosner, M.; Krupitza, G.; Hengstschläger, M.; Dolznig, H. In vitro cell migration and invasion assays. *Mutat. Res. Mutat. Res.* **2013**, *752*, 10–24. [CrossRef] [PubMed]
27. Goetsch, K.P.; Niesler, C.U. Optimization of the scratch assay for in vitro skeletal muscle wound healing analysis. *Anal. Biochem.* **2011**, *411*, 158–160. [CrossRef]
28. Büth, H.; Luigi Buttigieg, P.; Ostafe, R.; Rehders, M.; Dannenmann, S.R.; Schaschke, N.; Stark, H.J.; Boukamp, P.; Brix, K. Cathepsin B is essential for regeneration of scratch-wounded normal human epidermal keratinocytes. *Eur. J. Cell Biol.* **2007**, *86*, 747–761. [CrossRef]
29. Wiegand, C.; Hipler, U.-C. Methods for the measurement of cell and tissue compatibility including tissue regeneration processes. *GMS Krankenhaushygiene Interdiszip.* **2008**, *3*, 1–9.
30. Penick, K.J.; Solchaga, L.A.; Berilla, J.A.; Welter, J.F. Performance of polyoxymethylene plastic (POM) as a component of a tissue engineering bioreactor. *J. Biomed. Mater. Res. Part A* **2005**, *75*, 168–174. [CrossRef]
31. Klepeis, V.E.; Weinger, I.; Kaczmarek, E.; Trinkaus-Randall, V. P2Y receptors play a critical role in epithelial cell communication and migration. *J. Cell. Biochem.* **2004**, *93*, 1115–1133. [CrossRef]
32. Chmielewski, S.; Olejnik, A.; Sikorski, K.; Pelisek, J.; Błaszczyk, K.; Aoqui, C.; Nowicka, H.; Zernecke, A.; Heemann, U.; Wesoly, J.; et al. STAT1-dependent signal integration between IFNγ and TLR4 in vascular cells reflect pro-atherogenic responses in human atherosclerosis. *PLoS ONE* **2014**, *9*, 1–26. [CrossRef]
33. Horckmans, M.; Robaye, B.; Léon-Gómez, E.; Lantz, N.; Unger, P.; Dol-Gleizes, F.; Clouet, S.; Cammarata, D.; Schaeffer, P.; Savi, P.; et al. P2Y4 nucleotide receptor: A novel actor in post-natal cardiac development. *Angiogenesis* **2012**, *15*, 349–360. [CrossRef] [PubMed]
34. McClendon, J.; Jansing, N.L.; Redente, E.F.; Gandjeva, A.; Ito, Y.; Colgan, S.P.; Ahmad, A.; Riches, D.W.H.; Chapman, H.A.; Mason, R.J.; et al. Hypoxia-Inducible Factor 1α Signaling Promotes Repair of the Alveolar Epithelium after Acute Lung Injury. *Am. J. Pathol.* **2017**, *187*, 1772–1786. [CrossRef] [PubMed]
35. Hirano, Y.; Yasuma, T.; Mizutani, T.; Fowler, B.J.; Tarallo, V.; Yasuma, R.; Kim, Y.; Bastos-Carvalho, A.; Kerur, N.; Gelfand, B.D.; et al. IL-18 is not therapeutic for neovascular age-related macular degeneration. *Nat. Med.* **2014**, *20*, 1372–1375. [CrossRef] [PubMed]
36. Kaebisch, C.; Schipper, D.; Babczyk, P.; Tobiasch, E. The role of purinergic receptors in stem cell differentiation. *Comput. Struct. Biotechnol. J.* **2015**, *13*, 75–84. [CrossRef] [PubMed]
37. Babczyk, P.; Conzendorf, C.; Klose, J.; Schulze, M.; Harre, K.; Tobiasch, E. Stem Cells on Biomaterials for Synthetic Grafts to Promote Vascular Healing. *J. Clin. Med.* **2014**, *3*, 39–87. [CrossRef]
38. Zippel, N.; Limbach, C.A.; Ratajski, N.; Urban, C.; Luparello, C.; Pansky, A.; Kassack, M.U.; Tobiasch, E. Purinergic Receptors Influence the Differentiation of Human Mesenchymal Stem Cells. *Stem Cells Dev.* **2011**, *21*, 884–900. [CrossRef]
39. Hielscher, D.; Kaebisch, C.; Braun, B.J.V.; Gray, K.; Tobiasch, E. Stem Cell Sources and Graft Material for Vascular Tissue Engineering. *Stem Cell Rev. Reports* **2018**, *14*, 642–667. [CrossRef]
40. Zhang, Y.; Khan, D.; Delling, J.; Tobiasch, E. Mechanisms underlying the osteo- and adipo-differentiation of human mesenchymal stem cells. *Sci. World J.* **2012**, *2012*, 793823. [CrossRef]
41. Seifert, A.; Werheid, D.F.; Knapp, S.M.; Tobiasch, E. Role of Hox genes in stem cell differentiation. *World J. Stem Cells* **2015**, *7*, 583. [CrossRef]
42. Tobiasch, E. Differentiation Potential of Adult Human Mesenchymal Stem Cells. In *Stem Cell Engineering*; Springer: Berlin/Heidelberg, Germany, 2011; pp. 61–77.
43. Setiawan, M.; Tan, X.-W.; Goh, T.-W.; Hin-Fai Yam, G.; Mehta, J.S. Inhibiting glycogen synthase kinase-3 and transforming growth factor-β signaling to promote epithelial transition of human adipose mesenchymal stem cells. *Biochem. Biophys. Res. Commun.* **2017**, *490*, 1381–1388. [CrossRef]
44. Ramenzoni, L.; Weber, F.; Attin, T.; Schmidlin, P. Cerium Chloride Application Promotes Wound Healing and Cell Proliferation in Human Foreskin Fibroblasts. *Materials (Basel)* **2017**, *10*, 573. [CrossRef] [PubMed]
45. Park, H.J.; Salem, M.; Semlali, A.; Leung, K.P.; Rouabhia, M. Antimicrobial peptide KSL-W promotes gingival fibroblast healing properties in vitro. *Peptides* **2017**, *93*, 33–43. [CrossRef] [PubMed]
46. Scheiblich, H.; Roloff, F.; Singh, V.; Stangel, M.; Stern, M.; Bicker, G. Nitric oxide/cyclic GMP signaling regulates motility of a microglial cell line and primary microglia in vitro. *Brain Res.* **2014**, *1564*, 9–21. [CrossRef] [PubMed]

47. Mavi, M.F.; Ji, J.Y. Endothelial wound recovery is influenced by treatment with shear stress, wound direction, and substrate. *Cell. Mol. Bioeng.* **2013**, *6*, 310–325. [CrossRef]
48. Lin, X.; Helmke, B.P. Cell structure controls endothelial cell migration under fluid shear stress. *Cell. Mol. Bioeng.* **2009**, *2*, 231–243. [CrossRef]
49. Kang, Z.; Zhu, H.; Jiang, W.; Zhang, S. Protocatechuic acid induces angiogenesis through PI3K-Akt-eNOS-VEGF signalling pathway. *Basic Clin. Pharmacol. Toxicol.* **2013**, *113*, 221–227. [CrossRef]
50. De Jong, E.K.; Breukink, M.B.; Schellevis, R.L.; Bakker, B.; Mohr, J.K.; Fauser, S.; Keunen, J.E.E.; Hoyng, C.B.; Den Hollander, A.I.; Boon, C.J.F. Chronic central serous chorioretinopathy is associated with genetic variants implicated in age-related macular degeneration. *Ophthalmology* **2015**, *122*, 562–570. [CrossRef]
51. Zhou, Y.; Li, S.; Li, J.; Wang, D.; Li, Q. Effect of microRNA-135a on Cell Proliferation, Migration, Invasion, Apoptosis and Tumor Angiogenesis Through the IGF-1/PI3K/Akt Signaling Pathway in Non-Small Cell Lung Cancer. *Cell. Physiol. Biochem.* **2017**, *42*, 1431–1446. [CrossRef]
52. Lin, P.-Y.; Sung, P.-H.; Chung, S.-Y.; Hsu, S.-L.; Chung, W.-J.; Sheu, J.-J.; Hsueh, S.-K.; Chen, K.-H.; Wu, R.-W.; Yip, H.-K. Hyperbaric Oxygen Therapy Enhanced Circulating Levels of Endothelial Progenitor Cells and Angiogenesis Biomarkers, Blood Flow, in Ischemic Areas in Patients with Peripheral Arterial Occlusive Disease. *J. Clin. Med.* **2018**, *7*, 548. [CrossRef]
53. Stoeckius, M.; Erat, A.; Fujikawa, T.; Hiromura, M.; Koulova, A.; Otterbein, L.; Bianchi, C.; Tobiasch, E.; Dagon, Y.; Sellke, F.W.; et al. Essential roles of Raf/extracellular signal-regulated kinase/mitogen- activated protein kinase pathway, YY1, and Ca2+ influx in growth arrest of human vascular smooth muscle cells by bilirubin. *J. Biol. Chem.* **2012**, *287*, 15418–15426. [CrossRef]
54. Liebert, M.A.; Soares, M.P.; Usheva, A.; Brouard, S.; Berberat, P.O.; Gunther, L.; Tobiasch, E.; Bach, F.H. Heme Oxygenase-1-Derived Carbon Monoxide. *J. Biol. Chem.* **2002**, *277*, 17950–17961.
55. Brouard, S.; Berberat, P.O.; Tobiasch, E.; Seldon, M.P.; Bach, F.H.; Soares, M.P. Heme oxygenase-1-derived carbon monoxide requires the activation of transcription factor NF-κB to protect endothelial cells from tumor necrosis factor-α-mediated apoptosis. *J. Biol. Chem.* **2002**, *277*, 17950–17961. [CrossRef] [PubMed]
56. Brouard, S.; Otterbein, L.E.; Anrather, J.; Tobiasch, E.; Bach, F.H.; Choi, A.M.; Soares, M.P. Carbon monoxide generated by heme oxygenase 1 suppresses endothelial cell apoptosis [In Process Citation]. *J. Exp. Med.* **2000**, *192*, 1015–1026. [CrossRef] [PubMed]
57. Pinto, B.I.; Cruz, N.D.; Lujan, O.R.; Propper, C.R.; Kellar, R.S. In Vitro Scratch Assay to Demonstrate Effects of Arsenic on Skin Cell Migration. *J. Vis. Exp.* **2019**, *144*, e58838. [CrossRef] [PubMed]
58. Carr, J.J.; Brown, J.M.; John, M. *Introduction to Biomedical Equipment Technology*; Prentice Hall: Upper Saddle River, NJ, USA, 2001; ISBN 0130104922.
59. Yue, P.Y.K.; Leung, E.P.Y.; Mak, N.K.; Wong, R.N.S. A Simplified Method for Quantifying Cell Migration/Wound Healing in 96-Well Plates. *J. Biomol. Screen.* **2010**, *15*, 427–433. [CrossRef] [PubMed]
60. Jonkman, J.E.N.; Cathcart, J.A.; Xu, F.; Bartolini, M.E.; Amon, J.E.; Stevens, K.M.; Colarusso, P. An introduction to the wound healing assay using live-cell microscopy. *Cell Adhes. Migr.* **2014**, *8*, 440–451. [CrossRef] [PubMed]
61. Breiman, L. Random Forests. *UC Berkeley* **1999**, *TR567*, 1–35.
62. Obulkasim, A.; Meijer, G.A.; van de Wiel, M.A. Stepwise classification of cancer samples using clinical and molecular data. *BMC Bioinformatics* **2011**, *12*, 422–434. [CrossRef]